Transverse momentum of ionized atoms and diatomic molecules acquired in collisions with fast highly-charged heavy ion

V. Horvat and R. L. Watson

The momenta of ions and electrons emerging from collisions between charged projectiles and neutral target atoms or molecules have been topics of interest over the past few decades. However, precise simultaneous measurements of all three individual vector components of momentum for charged recoil ions produced in the collisions became possible more recently, following the development of recoil-ion momentum spectrometers (RIMS) that incorporated fast timing and simultaneous two-dimensional position determination capabilities. The high resolution, high efficiency, and reliability of RIMS's is accomplished by combining large-area microchannel plate detectors with delay-line anodes, high-precision time digitizers, and advanced signal-reconstruction algorithms [1].

So far, it has been established [2-6] that ionizing collisions involving fast highly-charged heavy ions and neutral atoms having more than two electrons occur predominantly at large impact parameters and may result in single, double, or multiple ionization of the target atoms, thus turning them into charged recoil ions. Ionization of the target atoms is predominantly due to pure ionization, in which the projectile charge does not change. The resulting recoil-ion charge distribution is a steep monotonically decreasing function of charge [7], while the recoil-ion transverse momentum $q_\perp$ (perpendicular to the momentum of the incoming projectile) is relatively small for low-charged recoil ions (*i.e.* no more than a few atomic units), but increases rapidly as a function of recoil-ion charge [2-6]. This increase is a consequence of the fact that Coulomb interaction between the projectile and the recoil ion (after its formation) is stronger when the recoil-ion charge is higher and when the impact parameter is smaller. These two causes are related, since recoil ions with higher charge are generally produced in collisions characterized by smaller impact parameters.

The production of very high recoil-ion charge states at very small impact parameters is increasingly due to ionization accompanied by single, double or multiple electron transfer from the target to the projectile or single, double, or multiple projectile electron loss. The recoil-ion charge distributions resulting from these processes are generally bell-shaped [7].

However, there are no known reports of measured $q_\perp$ distributions in strong-interaction collisions between fast highly-charged heavy ions and molecules having more than two electrons. Presumably, the transverse momentum of molecular ions emerging from the collisions should have a distribution similar to that expected for ionized atomic targets having comparable charge-to-mass ratio, as long as the size of the molecule is much smaller than the impact parameter. However, this may not hold true for small-impact-parameter collisions that result in double or multiple target ionization, which in turn leads to the dissociation of molecules, predominantly into positively charged fragments.

In our experiment a RIMS system was used to detect recoil ions created by bombardment of Ne, Ar, CO, N_2, and O_2 gas targets by a beam of 2.5 MeV/u Xe^{13+} ions [8]. Regardless of the target used, the outgoing beam was found to consist of about 98 % Xe^{13+}, 1.3 % Xe^{12+}, and 0.3 % Xe^{14+}. The $q_\perp$ resolution was estimated as being better than 5 a.u..

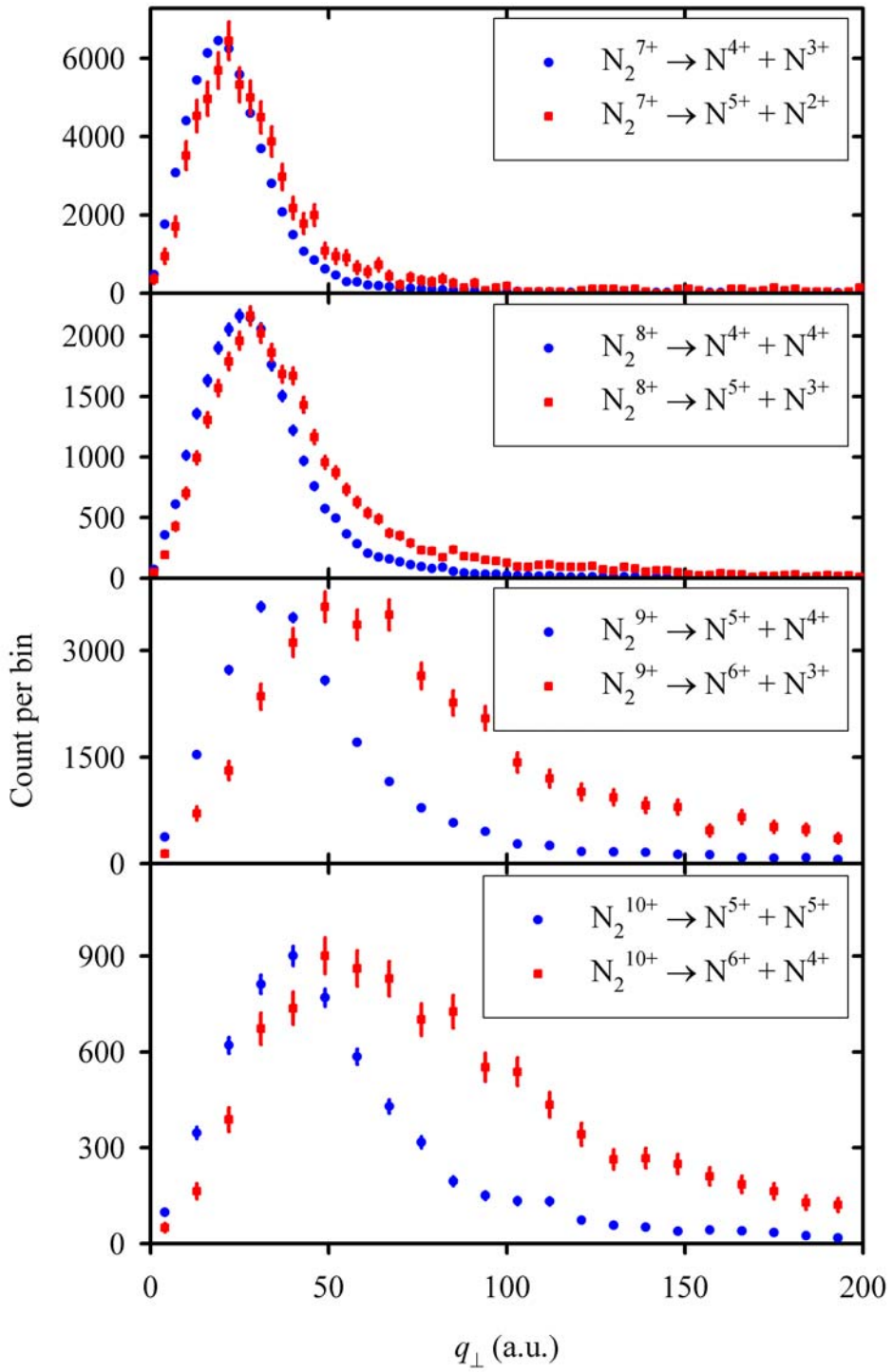

FIG. 1. Comparison of the $q_\perp$ distributions for dissociation channels corresponding to the same N_2 parent molecular ion, which is assumed to have charge number equal to the combined fragment charge numbers. In each plot, the number of counts per bin as indicated on the vertical axis scale applies to the dominant dissociation channel (*i.e.*, one that is listed first in the legend). Distributions for the remaining dissociation channels in each plot were scaled so that their maximum values match that of the corresponding dominant dissociation channel. The bin size is 3 a.u. for N_2^{7+} and N_2^{8+} and 9 a.u. for N_2^{9+} and N_2^{10+} parent molecular ions. The error bars shown are purely statistical.

Since in the strong interaction regime the duration of a collision (on the order of 10^{-17} s in the present case) is typically much shorter than the target relaxation time (on a time scale of 10^{-14} s in this work), it can be expected that target relaxation is virtually unaffected by the projectile. Consequently, in the case of ionization of a diatomic molecule by a fast projectile, followed by the molecular dissociation into two positively charged fragments having charge numbers Q_1 and Q_2, it is expected that the $q_\perp$ distributions are essentially the same for all dissociation channels corresponding to the same combined fragment charge number $Q = Q_1 + Q_2$. An upward shift (*Q-shift*) of the distributions as Q increases is expected due to the fact that a parent molecular ion with a higher value of Q is more likely to be produced in a collision at a smaller impact parameter, which in turn is more likely to result in a larger transverse momentum of the target core due to the increased Coulomb interaction between these two collision partners.

Both of these expectations were confirmed to be true for values of $Q < 7$ for all three molecular targets used. However, for $Q \geq 7$, it was found that a more asymmetric dissociation channel (*i.e.*, one corresponding to a larger value of $| Q_1 - Q_2 |$) has a larger Q-shift compared to a less asymmetric dissociation channel (*i.e.*, one corresponding to a smaller value of $| Q_1 - Q_2 |$). The absolute difference between these Q-shifts was found to increase as Q increases. This is demonstrated in Fig. 1 for the case of N_2 molecular dissociation. This effect will be referred to as the *ΔQ-split* in the text that follows.

Moreover, Fig. 1 also shows that for $Q = 9$ and 10, the ΔQ-splits are much larger than those observed for $Q = 7$ and 8. Considering that the two more asymmetric dissociation channels for $Q = 9$ and 10 include a hydrogen-like N^{6+} ion, this effect is presumably due to the fact that in order to remove a tightly-bound nitrogen *K*-shell electron in addition to other more loosely-bound electrons, a significant increase in the ionization potential must be overcome, for which the average impact parameter must decrease more drastically than is required for the removal of a less tightly bound electron. The same argument also helps explain why the less asymmetric dissociation channel is the dominant one.

For $Q = 9$ and 10, the $q_\perp$ distributions for the dissociation channels involving an N^{6+} ion, compared to the other two distributions, also have significantly longer tails, well beyond what could be expected based on the overall upward shift of the distributions (the ΔQ-split), which includes the upward shift of the distributions' peak values. This additional has a different character than that of the ΔQ-split and will be referred to as the *tail effect* in the text that follows. The onset of the tail effect at $Q = 8$ is most likely related to the increased importance of a different ionization mechanism involving target-to-projectile electron transfer, which is known to become increasingly important for the production of highly charged recoils [7] and also for the removal of tightly-bound target electrons. Therefore, the tail effect could be explained by the difference between the impact parameter *distribution* of pure ionization (which in the present case is dominant for $Q \leq 7$) and that of ionization accompanied by electron transfer from the target to the projectile (which in the present case becomes apparent at $Q \geq 8$ when the target starts losing its tightly-bound electrons).

The $q_\perp$ distributions for N_2 and CO molecular ions dissociating into positively charged fragments, as a function of the combined fragment charge number $Q \leq 7$, are compared in Fig. 2, in which contributions from dissociation channels corresponding to the given combined charge are added together. Apparently, there is hardly any significant difference between any two distributions shown in

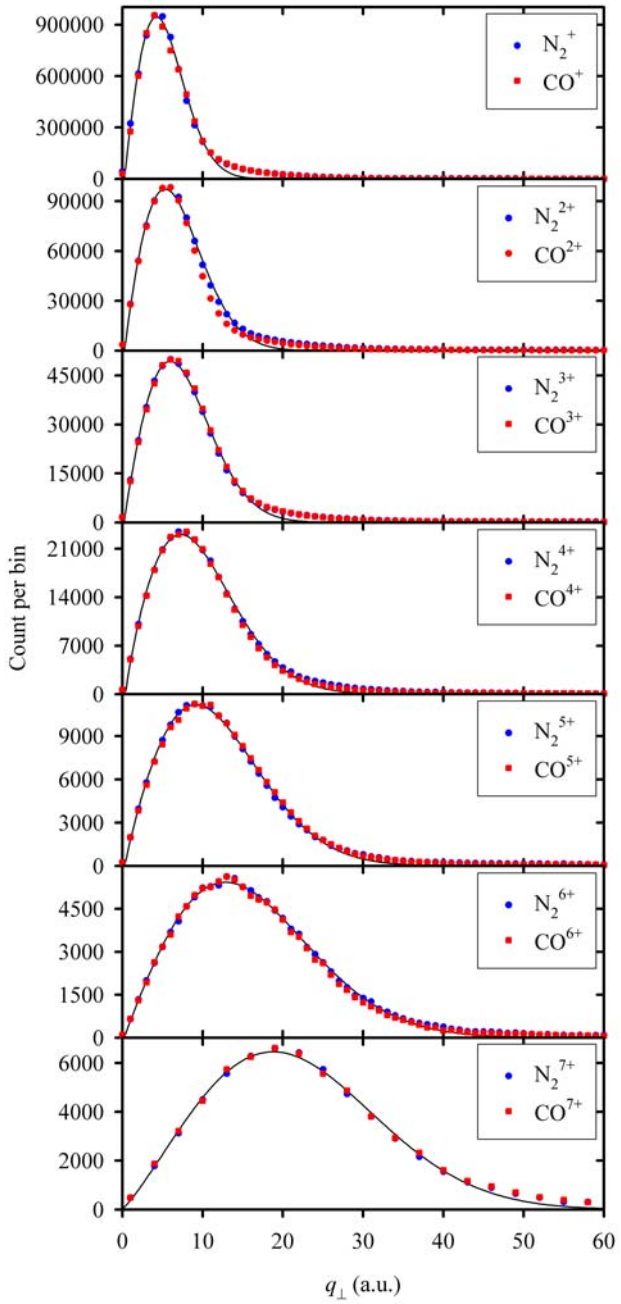

FIG. 2. Comparison of the $q\perp$ distributions for N_2 and CO molecular ions dissociating into positively charged fragments, as a function of the combined fragment charge number. Contributions from the dissociation channels corresponding to the given combined charge were added together. In each plot, the number of counts per bin as indicated on the vertical axis scale applies to the case of N_2. The distribution corresponding to CO in each plot was scaled so that the two maximum values match. The bin size is 3 a.u. for CO^{7+} and N_2^{7+} and 1 a.u. for the remaining parent molecular ions. The statistical error bars are not visible because they are smaller than the symbol size. The parent molecular ion's charge state listed in the legend is assigned the value equal to the combined fragment charge number. For completeness, also included is a plot showing the $q\perp$ distributions for non-dissociated N_2^+ and CO^+ molecular ions. The solid lines represent the overall fit of the distributions for N_2^{Q+} (parent) molecular ions ($Q \leq 7$) using Weibull functions.

the same plot. This can be expected based on the fact that the two molecules have the same combined atomic mass number and the same combined atomic number. However, N_2 and CO also have significantly different distributions of their excited states, which is evidenced by the significantly different kinetic-energy release (KER) spectra for doubly and triply charged molecular ions, as shown in Figs. 3 and 5 of Ref. [8]. This implies that, as long as tightly-bound electrons are not removed, or as long as pure ionization is the dominant mechanism for electron removal, the electronic or molecular structure of the target does not significantly affect the $q_\perp$ distribution.

Also included in Fig. 2 is a plot showing the $q_\perp$ distributions for non-dissociated N_2^+ and CO^+ molecular ions, which shows that the transverse momentum resolution in the present work is about 5 a.u. or better, as expected considering that a skimmer-collimated effusive gas jet was used [3].

All of the measured $q_\perp$ distributions were fitted with a four-parameter Weibull function. The results for N_2^{Q+} (parent) molecular ions ($Q \leq 7$) are shown by the solid lines in Fig. 2. Apparently, Weibull functions represent the shapes of the $q_\perp$ distributions very well, with only minor discrepancies at the tail for $Q \leq 3$. A similar quality of fit was obtained for all the other $q_\perp$ distributions. By restricting the region of fit to the area around the peak of the distribution (typically the region covered by the full width at half maximum), best estimates of the peak positions $q_\perp^0$ could be determined precisely and in a consistent way.

Since periods of rotation for the diatomic molecules used in this work are on the order of 10^{-12} s, while molecular fragmentation resulting from Coulomb explosions of the multi-charged molecular ions occurs on a much shorter time scale (of 10^{-14} s), it may be assumed that the orientation of the molecular axis remains unchanged between the time just prior to the collision and the end of the dissociation process. Therefore, it also may be assumed that orientation of the target molecule at the time of collision is defined by the momentum vector of its charged fragments during dissociation.

It is expected that orientation of the target molecule at the time of collision does not affect $q_\perp$ as long as the impact parameter is significantly larger than the size of the molecule. This condition is fulfilled for the majority of collisions that result in the removal of only a small number (or fraction) of electrons from the target. On the other hand, most close collisions result in the removal of a large fraction of electrons from the target and the process might be expected to have some dependence on the molecular orientation. Specifically, if the target molecule is initially oriented in the longitudinal direction, the impact parameters for two atomic centers are similar and the collision is expected to result in a symmetric or nearly-symmetric charge distribution between the atomic centers of the molecule. On the other hand, if the target molecule is initially oriented in the transverse direction, the impact parameters for two atomic centers are significantly different and the collision is expected to result in a highly asymmetric charge distribution. Therefore, the dissociation channels characterized by highly asymmetric charge distributions between the atomic centers are expected to have angular distributions that are enhanced in the transverse direction, while the dissociation channels characterized by symmetric or nearly-symmetric charge distributions are expected to have angular distributions that are suppressed in the transverse direction.

As expected, no conclusive evidence was found of anisotropy in the distributions of fragment pairs from low-charged molecular ions. However, for the symmetric and the nearly-symmetric dissociation channels (*i.e.*, those corresponding to $|Q_1 - Q_2| \leq 1$), the fragments with combined charge

number Q exceeding 9 for N_2 and 10 for O_2 were found to be distributed with a reduced probability at angles α close to 90° relative to the beam direction, as illustrated in Fig. 3. Furthermore, the effect was found to become more significant as Q increases. Interestingly, the magnitude of the effect seems to

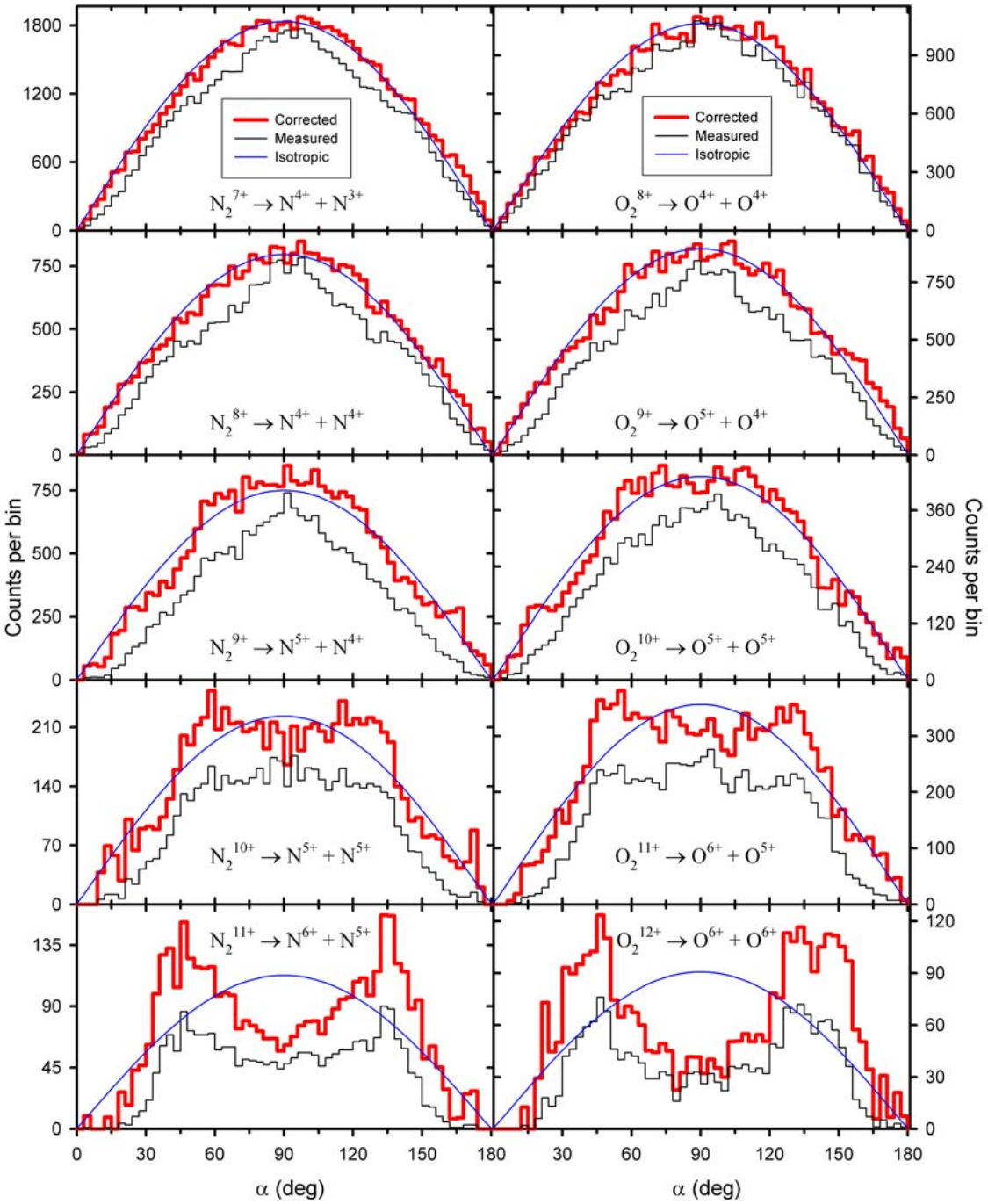

FIG. 3. Distributions of the numbers of correlated charged N_2 and O_2 molecular fragment pairs for the dissociation channels as indicated by the labels, shown as a function of angle α between the molecular axis at the time of collision and the beam direction. The thin (black) line represents the histogram of raw data, while the histogram shown with the thick (red) line is obtained by correcting the raw data for efficiency and fragment-pair acceptance of the apparatus, as described in detail in Ref.[8]. The smooth thin (blue) line shows the ideal isotropic distribution for the corrected total number of events. The N_2 and O_2 molecular ions in each row have the same value of Δn.

depend on Δn, the number of electrons removed *in addition* to one half of the number of available electrons ($\Delta n = Q - Z$). Consequently, the plots shown in Fig. 3 are selected and arranged so that each row corresponds to a given number $Q - Z$, where Z is the atomic number of nitrogen (in the first column) or oxygen (in the second column).

For highly asymmetric dissociation channels (*i.e.*, those corresponding to $|Q_1 - Q_2| \geq 2$) usable experimental results (selectively shown in Fig. 4) are limited to the cases with $Q < 11$, due to the fact that

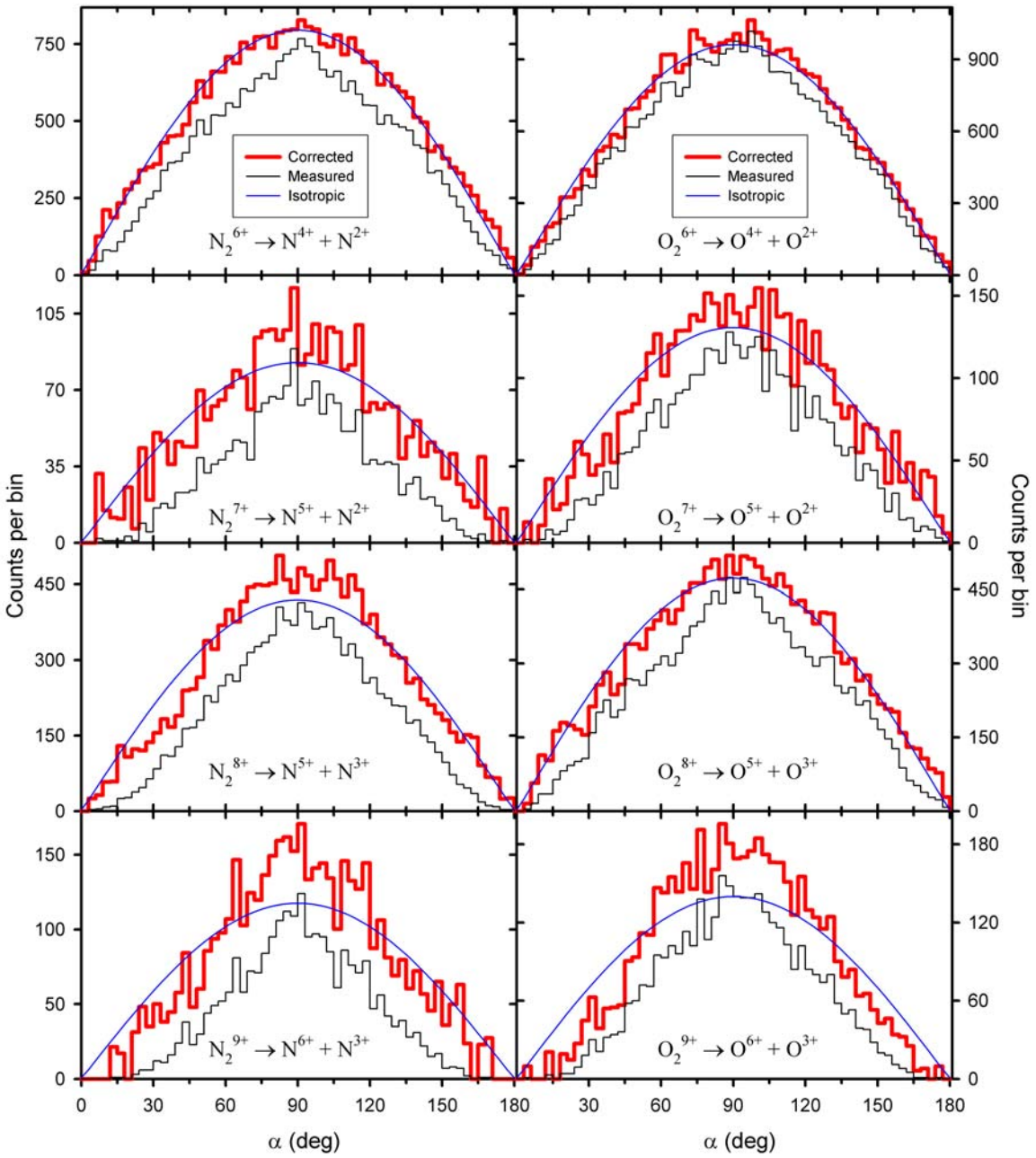

FIG. 4. Caption identical to that of Fig. 3 applies.

the production cross section decreases as Q increases and the fact that the predominant dissociation channels are symmetric or nearly symmetric. Also, the highest observed fragment charge number was 6. A

higher fragment charge would require *K*-shell ionization of oxygen or double *K*-shell ionization of nitrogen, for which the cross section is relatively low due to the relatively high binding energy of the *K* electrons. Nevertheless, the angular distributions shown in Fig. 4 for $Q = 9$ are slightly different than those shown in Fig. 3 for the same value of Q, indicating that the fragments of highly-charged molecular ions may be distributed with an *enhanced* probability at angles α close to 90^o relative to the beam direction.

The onset of the observed angular anisotropy may also be affected by the charge redistribution between the molecular fragments that may occur during dissociation and by autoionization, which is more likely to affect the fragment having lower charge (*i.e.*, more electrons). Both effects are likely to lead to charge equalization, which in effect makes an event from a more asymmetric dissociation channel appear in a less asymmetric (and more prominent) dissociation channel. Due to the apparent complementary properties of the angular distributions for these two dissociation channels (as described above), such events could make the angular distribution of the latter dissociation channel appear less anisotropic, thus shifting the onset of the observed anisotropy to higher values of Q.

As Q becomes large, autoionization becomes less likely because of the smaller number of available electrons and higher electronic binding energies, while charge redistribution may require tunneling of the electrons through the potential barrier between the atomic centers, which occurs with a drastically reduced probability. It can be estimated that the potential barrier of an electron transferring from N^{3+} to N^{6+} (about 80 eV) is only slightly higher than the ionization potential of N^{3+} (about 77 eV), which would imply that charge redistribution is unlikely for $Q > 9$. The reduced probability of charge equalization for $Q > 9$ coincides with the seeming onset of the deviations from an isotropic distribution, as shown in Figs. 3 and 4.

The effect of molecular orientation on $q_\perp$ distributions was found to be small. Consequently, the angular scale was reduced to only two bins; one covering $60^o \leq \alpha \leq 120^o$ and the other covering the remainder of the angular range, so that $|\cos\alpha| \leq 0.5$ in the former case and $|\cos\alpha| > 0.5$ in the latter case. For an isotropic angular distribution the two cases are expected to correspond to the same number of events. The results for the symmetric and nearly-symmetric dissociation channels are shown in Fig. 5. Apparently, the molecular orientation at the time of collision does have an effect on the $q_\perp$ distributions for $Q - Z > 0$ and its magnitude seems to depend on $Q - Z$. This effect was not present for the observed highly asymmetric dissociation channels.

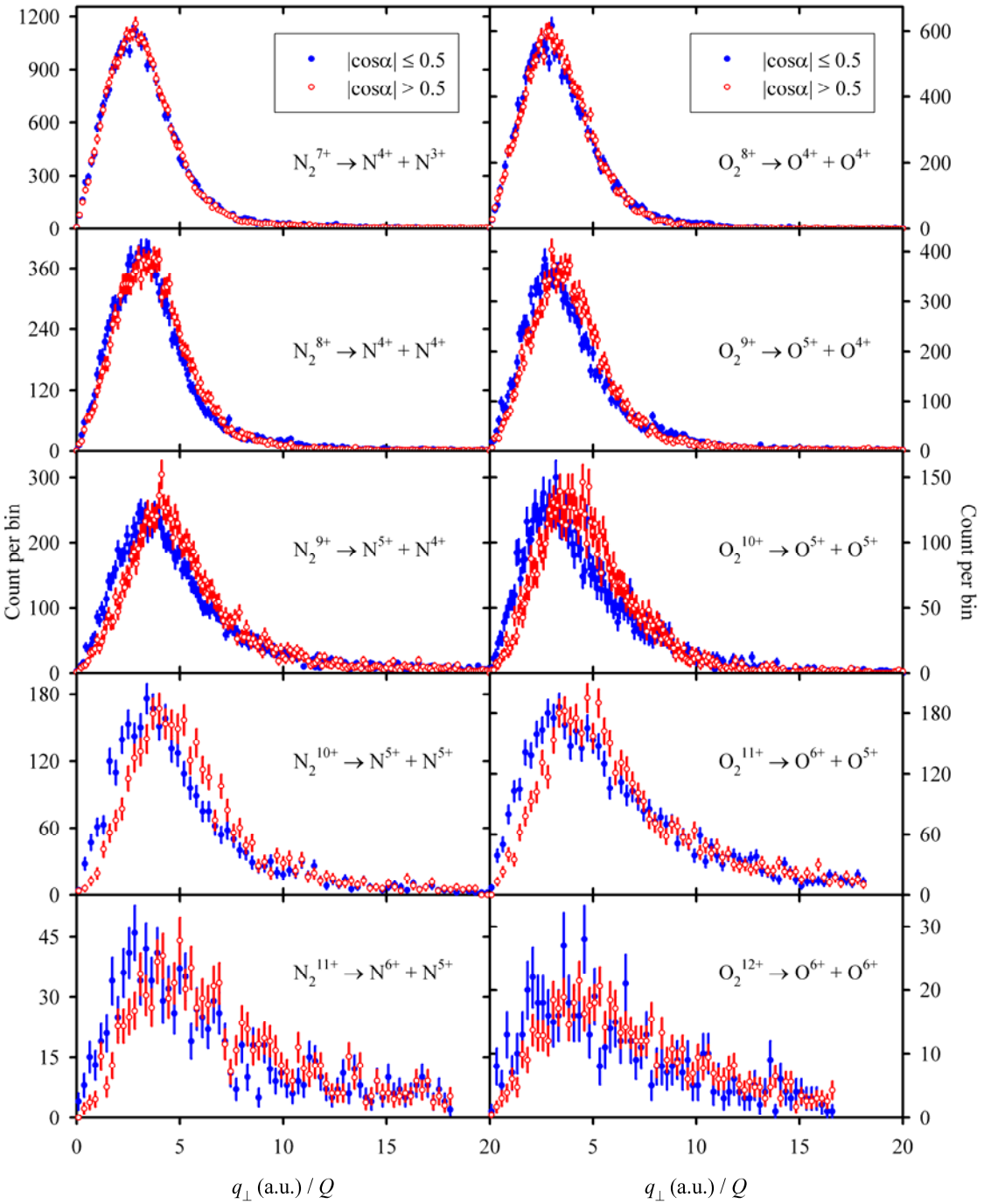

FIG. 5. Measured $q_{\perp}$ distributions for the selected N_2 and O_2 dissociation channels (as indicated by the labels) for angles $60^{o} \leq \alpha \leq 120^{o}$ ($|\cos\alpha| \leq 0.5$) and for the remainder of the angular range ($|\cos\alpha| > 0.5$), as indicated by the legend. The latter distribution was normalized to the total number of events of the former distribution and the scaling on the horizontal axis (*i.e.*, division by Q) was applied to enhance the details.

[1] http://www.roentdek.com.
[2] C.L. Cocke and R.E. Olson, Phys. Rep. **205**,153 (1991).
[3] J. Ullrich, R. Moshammer, R. Dörner, O. Jagutzki, V. Mergel, H. Schmidt-Böcking, and L. Spielberger, J. Phys. B **30**, 2917 (1997).
[4] R. Dörner, V. Mergel, O. Jagutzki, L. Spielberger, J. Ullrich, R. Moshammer, and H. Schmidt-Böcking, Phys. Rep. **330**, 95 (2000).
[5] J. Ullrich, R. Moshammer, A. Dorn, R. Dörner, L.Ph.H. Schmidt, and H. Schmidt-Böcking, Rep. Prog. Phys. **66**, 1463 (2003).
[6] M. Schulz and D.H. Madison, International J. Mod. Phys. A **21**, 3649 (2006).
[7] T.J. Gray, C.L. Cocke, and E. Justiniano, Phys. Rev. A **22**, 849 (1980); Phys. Rev. A **53**, 2407 (1996).
[8] V. Horvat and R.L. Watson, Nucl. Instrum. Methods Phys. Res. **B269**, 2584 (2011).